Volume 12
Number 36
28 September 2020
Pages 18481-18990

Nanoscale

rsc.li/nanoscale

ISSN 2040-3372

ROYAL SOCIETY OF CHEMISTRY

COMMUNICATION
Xiaoxue Xu, Fan Wang *et al.*
Video-rate upconversion display from optimized lanthanide ion doped upconversion nanoparticles

NCNST

Nanoscale

ROYAL SOCIETY OF CHEMISTRY

COMMUNICATION

View Article Online
View Journal | View Issue

Cite this: *Nanoscale*, 2020, **12**, 18595

Received 19th April 2020,
Accepted 4th June 2020

DOI: 10.1039/d0nr03076g

rsc.li/nanoscale

Video-rate upconversion display from optimized lanthanide ion doped upconversion nanoparticles†

Laixu Gao,[a,b] Xuchen Shan,[b] Xiaoxue Xu, *[b] Yongtao Liu,[b] Baolei Liu,[b] Songquan Li,[a] Shihui Wen, [b] Chenshuo Ma,[b] Dayong Jin [b] and Fan Wang *[b,c]

Volumetric displays that create bright image points within a transparent bulk are one of the most attractive technologies in everyday life. Lanthanide ion doped upconversion nanoparticles (UCNPs) are promising luminescent nanomaterials for background free, full-colour volumetric displays of transparent bulk materials. However, video-rate display using UCNPs has been limited by their low emission intensity. Herein, we developed a video-rate upconversion display system with much enhanced brightness. The integral emission intensity of the single UCNPs was fully employed for video-rate display. It was maximized by optimizing the emitter concentration and, more importantly, by temporally synchronizing the scanning time of the excitation light to the the raised emission time of the single UCNPs. The excitation power dependent emission response and emission time decay curves were systematically characterized for the single UCNPs with various emitter concentrations from 0.5% to 6%. 1%Tm^{3+} doped UCNPs presented the highest integral emission intensity. By embedding this UCNPs into a polyvinyl acetate (PVA) film, we achieved a two-dimensional (2D) upconversion display with a frame rate of 29 Hz for 35 by 50 pixels. This work demonstrates that the temporal response as well as the integral emission intensity enable video-rate upconversion display.

Introduction

Three-dimensional (3D) real time display restoring in real space has increasingly attracted more attention. A substantial variety of 3D optical display schemes have emerged recently, however, most electronic products display in 2D and pseudo-3D depending on the parallax used to differentiate the images. Besides this, research has also focused on grating[1,2] and optical tweezers[3,4] methods for 3D display. These systems are too complicated and their display ranges are limited. 3D displays based on lanthanide ion doped upconversion nanoparticles (UCNPs)[5] has become an emerging field, due to their unique photonic properties. With the ladder-like 4f energy configurations[6,7] of Ln ions, UCNPs can up-convert two or more lower-energy photons into one high-energy photon and emit visible and UV light[8–10] with a large anti-Stokes shift, zero background noise,[11] long lifetime, and low excitation power density. Ln-UCNPs have been adopted for a broad range of applications,[12,13] such as bio-imaging,[14–16] fluorescence microscopy,[17–20] nanomedicine[21,22] and transparent displays.[23–26] Among these, volumetric displays using UCNPs are capable of producing true 3D images *via* the embedding of UCNPs within transparent materials, which are visible from all directions. Such displays presents high brightness,[27] color modulation,[8,28] multi-perspective display,[29–31] high spatial resolution and faster scanning frequency.[15–18]

However, video-rate upconversion display using UCNPs has not yet been achieved because it takes time for UNCPs to consecutively absorb two and more photons to emit high energy light, while at a high-speed scan frequency, there is not enough time for UCNPs to absorb sufficient photons to emit. Although increasing the excitation power can enhance the emission intensity of UCNPs with a higher concentration of emitters,[32,33] it is destructive to the display medium at high excitation power. Ideally for video-rate display, there is the requirement for UCNPs that can emit light with high intensity at low power excitation, and can response to excitation rapidly. To enable video-rate display using UCNPs, excitation power, emission intensity and response time should be considered at the same time.

In this work, we measured the integral emission intensity of single UCNPs to evaluate the photonic properties of the UCNPs for video-rate display. The integral luminescence of

[a]*School of Physical Science and Technology, Lingnan Normal University, Zhanjiang, 524048, China*
[b]*Institute for Biomedical Materials and Devices (IBMD), Faculty of Science, University of Technology Sydney, NSW 2007, Australia.*
E-mail: xiaoxuehelen.xu@uts.edu.au, Fan.wang@uts.edu.au
[c]*School of Electrical and Data Engineering, Faculty of Engineering and Information Technology, University of Technology Sydney, Ultimo 2007, Australia*
†Electronic supplementary information (ESI) available. See DOI: 10.1039/d0nr03076g

UCNPs is the emission intensity spanning from the increase in emission upon excitation, saturated emission and emission decay, which are related to the excitation power, response time and emission efficiency. To characterize the integral emission intensity, we built a laser scanning confocal microscopy system[34] to quantify the integral emission intensity, power dependent relationship and temporal domain behavior of the single UCNPs. A series of UCNPs, $NaYF_4$:20%Yb^{3+},x%Tm^{3+} (x = 0.5%, 1%, 2%, 4% and 6%), were synthesized and characterized systematically. The morphology observations measured using transmission electron microscopy (TEM) and the size distributions of the UCNPs are shown in Fig. S1 and S2,† respectively. The average sizes of the UCNPs are around 40 nm. It was found that the UCNPs with a high amount of Tm^{3+} doping showed high emission intensities but short lifetimes while the UCNPs with a low amount of Tm^{3+} doping exhibited low emission intensities but long lifetimes in the full emission spectra. Therefore, the critical concentration of Tm was found to be 1% with the UCNPs of $NaYF_4$:20%Yb^{3+},1% Tm^{3+} possessing the highest integral intensity under low power excitation. To maximize the integral emission intensity for the 1%Tm^{3+} doped UCNPs, the excitation beam scanning time matched the increased emission time of these UCNPs. We added the 1%Tm^{3+} doped UCNPs into a film made of polyvinyl acetate (PVA) and demonstrated the 2D video-rate display by naked eye using a home-built device that allows a laser to scan a pattern *via* an acousto-optic deflector. It could be expanded to a volumetric 3D display and wearable display using the optimized UCNPs.

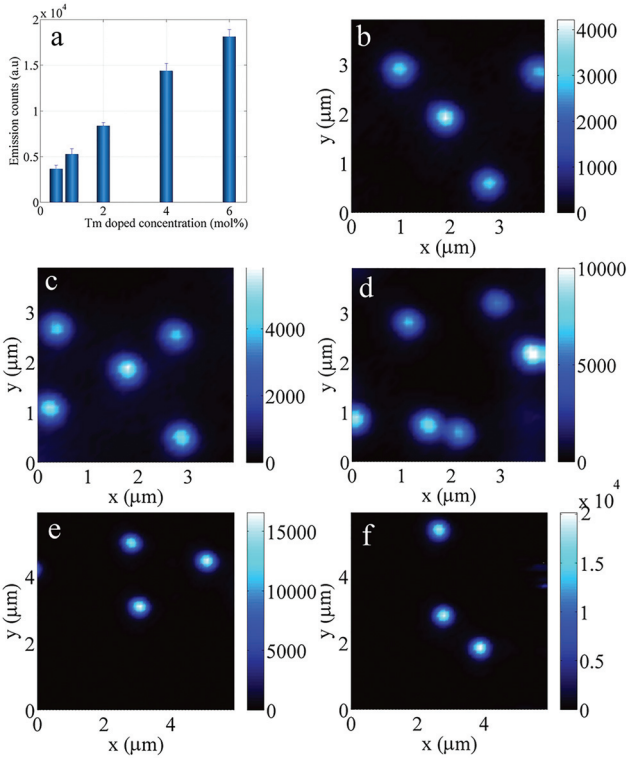

Fig. 1 Comparison of the emission luminescence intensity between single UCNPs with different Tm^{3+} doping concentrations with a power density of 80 MW cm^{-2}. (a) Average emission intensity of single nanoparticles with different Tm^{3+} doping concentrations. (b)–(f). Confocal images of single UCNPs with different Tm^{3+} doping concentrations of 0.5%, 1%, 2%, 4% and 6% mol.

Results and discussion

To comprehensively study the photonic properties of the UCNPs, we built a homemade laser scanning confocal microscopy system.[33] The advantage of this microscopy system is that it is an optical imaging technique to increase the optical resolution and contrast of a micrograph by means of using a spatial pinhole to block out-of-focus light during image formation.

We first compared the continuous emission intensity of single UCNPs using the home-built microscopy system. The synthesized UCNPs, $NaYF_4$:20%Yb^{3+},x%Tm^{3+}, (x = 0.5, 1, 2, 4 and 6) were in the size range of 20 to 40 nm. Fig. 1a shows the emission intensity of the single UCNPs with 0.5%Tm^{3+} to 6% Tm^{3+} at a high excitation power (of 80 MW cm^{-2}). The quantitative comparison was derived from the intensity calculation in the confocal imaging of the single UCNPs (Fig. 1b–f). For mono-dispersed UCNP samples in the confocal image, the intensity value of each Gaussian spot is uniform, representing one nanoparticle. Its maximum value of the intensity bar indicates the full emission intensity of the particle from all emission wavelengths. The emission intensity values at Tm^{3+} doping concentrations of 0.5%, 1%, 2%, 4% and 6% mol were averaged from at least 50 single UCNPs and plotted as a function of Tm^{3+} doping concentration (Fig. 1a), with average intensities of 3610, 5260, 8370, 14 300, and 18 100 counts, respectively.

From Fig. 1, it can be seen that the photon count for the UNCPs with 6%Tm^{3+} is 5 times higher than that of UCNPs with 0.5%Tm^{3+}. The quantitative comparison clearly shows that the overall emission intensity of the UCNPs increases with an increase in the Tm^{3+} ions doping concentration under the excitation power (80 MW cm^{-2}). However, the results do not suggest that the highly doped UCNPs (*e.g.* 6%Tm^{3+}) are the best candidate for video-rate displaying, as the highly doped UCNPs show a lower emission intensity under the excitation conditions (0 to 3.5 MW cm^{-2}) of the free-space laser scanning system.

For power dependent measurements, the luminescence intensity from the single UCNPs was collected using a SPAD (single-photon avalanche diode) when the excitation power density was increased. The luminescence intensity power dependent relationship is very important for practical display applications because it can be used to determine the emission intensity of the single UCNPs under the used excitation power density.

Fig. 2 shows the measured power dependent emission intensity for single UCNPs with different Tm^{3+} concentrations. These curves present the changing trends of the emission

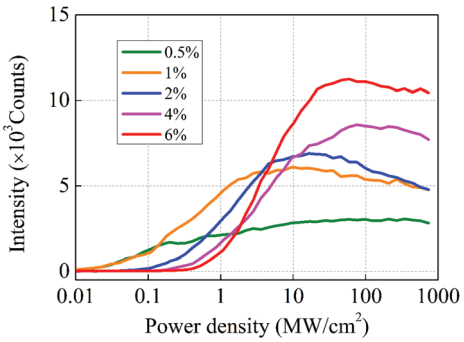

Fig. 2 Measured upconversion luminescence intensities of single UCNPs with different Tm^{3+} doping concentrations at different excitation power densities. Here, the intensity is the sum of the emission intensity for wavelengths in the range of 400–842 nm.

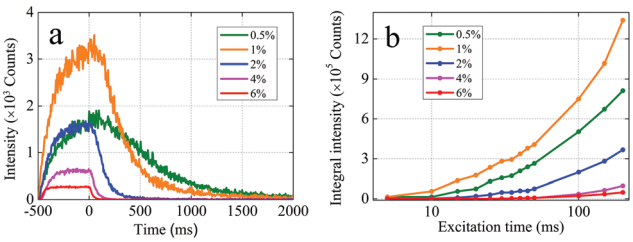

Fig. 3 (a) Rising times and lifetimes of single UCNPs with different Tm^{3+} doping concentrations under a power density of 0.48 MW cm^{-2}. (b) Trends and total emission intensity integrals of single UCNPs with different Tm^{3+} doping concentration changes according to excitation time.

intensities with the excitation power density of 980 nm light. It can be seen that the emission intensities of the UCNPs increase with an increase in the doping concentration in the range of high excitation power density from 10 to 700 MW cm^{-2}. At saturated excitation power density, more than enough photons can be absorbed by the sensitizer ions and transferred to a larger number of Tm^{3+} ions located closer to Yb^{3+} ions within $NaYF_4$:20%Yb^{3+},6%Tm^{3+}, therefore, the UCNPs with higher Tm^{3+} doping emitted higher luminescence intensity. While at low excitation power density (<~0.5 MW cm^{-2}), there might not be sufficient photons for the sensitizer to absorb and transfer to all of the Tm^{3+} ions for emission. Moreover, the high concentration of Tm^{3+} ions might also lead to them quenching each other during the energy transfer process, thus the 0.5% and 1%Tm^{3+} doped UCNPs appeared brighter at low excitation power. In the video rate display demonstration, we used a 980 nm laser and the calculated excitation power density focused on the UCNPs was 0.48 MW cm^{-2}. The luminescence intensity of the 6% doped samples was the lowest and the luminescence intensity of the 1% doped sample was the highest, at a power density of 0.48 MW cm^{-2}.

The lifetime under the excitation power density is usually desirable, because it determines the duration of the emission intensity. Before we arrive at the conclusion that the 1% doped UCNPs are the most suitable candidate as a material to be embedded in the scanning system, the time domain responses of the UCNPs have to be compared, since the beam scanning has to be synchronized with the time response of the UCNPs for optimized excitation efficiency. Fig. 3a shows the plots of the emission intensities of the single UCNPs *versus* the time-resolved emissions data, namely the excitation time and lifetime under the excitation power density of 0.48 MW cm^{-2}.

The luminescence emission process includes both the rising time, the plateau and the decay of the emission upon pulsed excitation using a 980 nm laser. The NIR laser was switched on at −500 μs and switched off at 0 μs. Here, the rising region is due to the energy transfer from the sensitizer ions (Yb^{3+}) to the emitter ions (Tm^{3+}), which could be characterized using the energy transfer rate. The decay region in the time resolved emission results from the carrier relaxation in the energy levels. A detailed explanation of this can be found in section 2 and Fig. S3 in the ESI.† It can be seen that at this low excitation power, the 1%Tm^{3+} doped UNCPs present the highest emission intensity while the 6%Tm^{3+} doped UCNPs exhibit the lowest emission intensity.

Moreover, the lifetimes were fitted and calculated from these plots, which showed that the 0.5%Tm^{3+} doped UCNPs exhibited an extremely long lifetime of 516 μs compared with values of 265, 98, 47 and 27 μs for the 1%, 2%, 4% and 6% Tm^{3+} doped UCNPs, respectively. Apparently, the lifetimes decreased upon an increase in theTm^{3+} doping concentration, probably due to the greater chance of cross relaxation with more Tm^{3+} ions.[35–37] Fig. 3b shows the integral emission intensity of the UCNPs. The integral emission intensity, calculated by integrating the lifetime response curve, including rising, stable and decay range, is proportional to the total photon number emitted by a single pixel. It is interesting to observe that the integral emission intensity of 1%Tm^{3+} doped UCNPs presents the highest integral emission intensity among all Tm^{3+} doping concentrations. This suggests that the brightness of 1%Tm^{3+} doped UCNPs make it the best candidate for upconversion display. It is worth noting that under 980 nm excitation, all visible light emitted from Tm^{3+} would contribute to the display brightness, so the full emission bands were taken into account for a bright display. Although the rising time of a specific emission band could be shorter than the total rising time of all emission bands, the scanning speed could be faster and more points could be displayed, with a substantial drop in the total emission intensity.

We further used the 1%Tm^{3+} doped UCNPs to demonstrate a video-rate upconversion display. The displaying system consists of a 980 nm laser, an acousto-optic deflector (AOD, DTSXY) controlled by a computer, a focusing lens and a screen film made of UCNPs doped with 1%Tm^{3+}, as shown in Fig. 4a.

The near-infrared laser beam passes through the AOD, and is focused on the UCNP display film. Fig. 4b and c show the excitation lens and the display film. Considering the intensity integral over excitation time, for a single pixel, the excitation time is longer, and the UCNP is brighter. Nevertheless, for a display array, a long excitation time for each pixel causes the

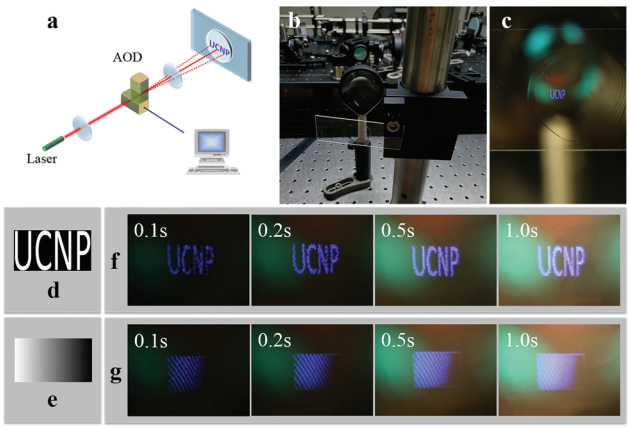

Fig. 4 (a) Schematic of the computer-controlled scanning system that employs AOD and an optical lens to control light deflection and focus. (b) Photograph of the display system. (c) The letters "UCNP" displayed on the PVA film. (d) The "UCNP" pattern and (e) grayscale gradient pattern entered by a computer. (f) "UCNP" pattern photographs and (g) greyscale gradient photographs taken at different exposure times (0.1, 0.2, 0.5, and 1.0 s).

scanning frequency to slow down and image display flashing, which makes the eyes strain and affects the display image quality. This puts forward a certain limit on the number of array points and scanning speed. On the premise of ensuring the sufficient display brightness of each pixel point, the scanning frequency should be increased as fast as possible, so that the image display does not flicker, and the number of the pattern dot matrix can also be set to the maximum value to make the display resolution higher. In order to ensure the continuity of the display, movie cameras typically operate at a speed of at least 24 frames per second. In this experiment, we set the scanning dot matrix to 35 × 50, and the patterns are the letters "UCNP" and a grey gradient square, as shown in Fig. 4d and e. With a 20 μs excitation time for each pixel and power density of 0.48 MW cm^{-2}, the upconversion luminescence was visible to the naked eye. The graphic images (Fig. 4f) of the letters "UCNP" and the square grey gradient images (Fig. 4g) were generated on the film with different exposure times. The images were recorded under ambient room lighting conditions and were also observed by the naked eye at the same pumping power, and the letters "UCNP" were clear and the grayscale gradient of the rectangular image could be distinguished at a frame rate of 29 Hz. At a short exposure time, the image was limited by the frame rate, showing obvious grains, and could be improved by reducing the scanning dot matrix or excitation time.

Conclusions

The key problems of video-rate upconversion displays are the luminescence response speed and luminance of the UCNPs. The emission intensities and lifetimes of single UCNPs with various Tm^{3+} doping concentrations were characterized. The emission intensities and time-resolved emissions of the samples showed that the doped UCNPs exhibited the increasing highest emission intensity but a decreasing lifetime for the fully emitted wavelength due to an increase in the Tm^{3+} doping concentration from 0.5% to 6%. Therefore, the integral emission intensity during the fluorescence lifetime should be considered for display. It was found that the 1%Tm^{3+} presented the shortest rising time and the highest integral emission intensity at a low excitation power of 0.48 MW cm^{-2}. The imaging rate can still be improved by further enhancing the emission intensity of the UCNPs under a lower excitation power, *e.g.* for a core shell structure. In this work, we demonstrated that the integrated luminescence and synchronization of scanning time with the emission rising time benefit video-rate upconversion display using UCNPs. Further comprehensive research on 3D upconversion displays will be highly useful for various fields and applications, such as wearable displays.

Conflicts of interest

There are no conflicts to declare.

Acknowledgements

This research is supported by the National Natural Science Foundation of China (No. 61905105), the Guangdong Science and Technology Innovation Strategy Project (2018A01006), and the Zhanjiang Science and Technology Project (2019A01044; 2019B01001). We would like to acknowledge the Australian Research Council DECRA fellowship (DE200100074 – F. W.), the Australian Research Council Discovery Projects, (DP190101058 – F. W.) and Chancellor Postdoctoral Fellowship at the University of Technology Sydney (X. X.).

References

1 T. Toda, S. Takahashi and F. Iwata, Symposium on Electronic Imaging, 1995, vol. 2406, pp. 191–198.
2 M. Petz and R. Ritter, *Int. Soc. Opt. Eng.*, 2001, **4399**, 35–41.
3 G. Carmon, I. Fishov and M. Feingold, *Opt. Lett.*, 2012, **37**, 440.
4 H. Mushfique, J. Leach, H. Yin, R. Di Leonardo, M. J. Padgett and J. M. Cooper, *Anal. Chem.*, 2008, **80**, 4237–4240.
5 A. Nadort, J. Zhao and E. M. Goldys, *Nanoscale*, 2016, **8**, 13099–13130.
6 X. Xu, C. Clarke, C. Ma, G. Casillas, M. Das, M. Guan, D. Liu, L. Wang, A. Tadich, Y. Du, C. Ton-That and D. Jin, *Nanoscale*, 2017, **9**, 7719–7726.
7 H. Zhang, Y. Li, Y. Lin, Y. Huang and X. Duan, *Nanoscale*, 2011, **3**, 963–966.
8 C. Zhang, L. Yang, J. Zhao, B. Liu, M. Y. Han and Z. Zhang, *Angew. Chem., Int. Ed.*, 2015, **54**, 11531–11535.
9 F. Wang and X. Liu, *Acc. Chem. Res.*, 2014, **47**, 1378–1385.

10 S. Sivakumar, F. C. J. M. Van Veggel and M. Raudsepp, *J. Am. Chem. Soc.*, 2005, **127**, 12464–12465.
11 H. L. Jo, Y. H. Song, J. Park, E. J. Jo, Y. Goh, K. Shin, M. Kim and K. T. Lee, *Nanoscale*, 2015, **7**, 19397.
12 B. Zhou, B. Shi, D. Jin and X. Liu, *Nat. Nanotechnol.*, 2015, **10**, 924–936.
13 K. Zheng, K. Y. Loh, Y. Wang, Q. Chen, J. Fan, T. Jung, S. H. Nam, Y. D. Suh and X. Liu, *Nano Today*, 2019, **29**, 100797.
14 F. Wang, S. Wen, H. He, B. Wang, Z. Zhou, O. Shimoni and D. Jin, *Light: Sci. Appl.*, 2018, **7**, 18007.
15 Y. Liu, F. Wang, H. Lu, G. Fang, S. Wen, C. Chen, X. Shan, X. Xu, L. Zhang, M. Stenzel and D. Jin, *Small*, 2020, **16**, 1905572.
16 B. Liu, C. Chen, X. Di, J. Liao, S. Wen, Q. P. Su, X. Shan, Z. Xu, L. A. Ju, C. Mi, F. Wang and D. Jin, *Nano Lett.*, 2020, DOI: 10.1021/acs.nanolett.0c00448.
17 C. Chen, F. Wang, S. Wen, Q. P. Su, M. C. L. Wu, Y. Liu, B. Wang, D. Li, X. Shan, M. Kianinia, I. Aharonovich, M. Toth, S. P. Jackson, P. Xi and D. Jin, *Nat. Commun.*, 2018, **9**, 4–9.
18 Y. Liu, Y. Lu, X. Yang, X. Zheng, S. Wen, F. Wang, X. Vidal, J. Zhao, D. Liu, Z. Zhou, C. Ma, J. Zhou, J. A. Piper, P. Xi and D. Jin, *Nature*, 2017, **543**, 229–233.
19 X. Peng, B. Huang, R. Pu, H. Liu, T. Zhang, J. Widengren, Q. Zhan and H. Agren, *Nanoscale*, 2019, **11**, 1563–1569.
20 B. Huang, Q. Wu, X. Peng, L. Yao, D. Peng and Q. Zhan, *Nanoscale*, 2018, **10**, 21025–21030.
21 W. Fan, W. Bu and J. Shi, *Adv. Mater.*, 2016, **28**, 3987–4011.
22 J. Xu, A. Gulzar, D. Yang, S. Gai, F. He and P. Yang, *Nanoscale*, 2019, **11**, 17535–17556.
23 E. Downing, L. Hesselink, J. Ralston and R. Macfarlane, *Science*, 2016, **273**, 1185–1189.
24 S. Wen, J. Zhou, K. Zheng, A. Bednarkiewicz, X. Liu and D. Jin, *Nat. Commun.*, 2018, **9**, 2415.
25 B. J. Park, A. R. Hong, S. Park, K. U. Kyung, K. Lee and H. S. Jang, *Sci. Rep.*, 2017, **7**, 1–12.
26 B. Koudsi, H. Refai and J. J. Sluss, *J. Disp. Technol.*, 2015, **11**, 266–272.
27 G. Chen, T. Y. Ohulchanskyy, R. Kumar, H. Ågren and P. N. Prasad, *ACS Nano*, 2010, **4**, 3163–3168.
28 R. Deng, F. Qin, R. Chen, W. Huang, M. Hong and X. Liu, *Nat. Nanotechnol.*, 2015, **10**, 237–242.
29 A. Rapaport, J. Milliez, M. Bass, A. Cassanho and H. Jenssen, *J. Disp. Technol.*, 2006, **2**, 68–78.
30 B. Zhu, B. Qian, Y. Liu, C. Xu, C. Liu, Q. Chen, J. Zhou, X. Liu and J. Qiu, *NPG Asia Mater.*, 2017, **9**, e394.
31 M. You, M. Lin, S. Wang, X. Wang, G. Zhang, Y. Hong, Y. Dong, G. Jin and F. Xu, *Nanoscale*, 2016, **8**, 10096–10104.
32 J. Zhao, D. Jin, E. P. Schartner, Y. Lu, Y. Liu, A. Zvyagin, L. Zhang, J. M. Dawes, P. Xi, J. A. Piper, E. M. Goldys and T. M. Monro, *Nat. Nanotechnol.*, 2013, **8**, 729–734.
33 C. Ma, X. Xu, F. Wang, Z. Zhou, D. Liu, J. Zhao, M. Guan, C. I. Lang and D. Jin, *Nano Lett.*, 2017, **17**, 2858.
34 X. Xu, Z. Zhou, Y. Liu, S. Wen, Z. Guo, L. Gao and F. Wang, *APL Photonics*, 2019, **4**, 026104.
35 Q. Zhan, H. Liu, B. Wang, Q. Wu, R. Pu, C. Zhou, B. Huang, X. Peng, H. Ågren and S. He, *Nat. Commun.*, 2017, **8**, 1–11.
36 B. Xue, D. Wang, Y. Zhang, J. Zuo, Y. Chang, L. Tu, X. Liu, Z. Yuan, H. Zhao, J. Song, J. Qu and X. Kong, Regulating the color output and simultaneously enhancing the intensity of upconversion nanoparticles via a dye sensitization strategy, *J. Mater. Chem. C*, 2019, **7**, 8607–8615.
37 Q. Shao, G. Zhang, L. Ouyang, Y. Hu, Y. Dong and J. Jiang, Emission color tuning of core/shell upconversion nanoparticles through modulation of laser power or temperature, *Nanoscale*, 2017, **9**, 12132–12141.